Journal of the European Ceramic Society **19** (1999) 2073–2077

PII: S0955-2219(99)00034-5
0955-2219/99/$ - see front matter

Microstructural Development in Pure and V-doped SnO_2 Nanopowders

L. Sangaletti,[a]* L. E. Depero,[a] B. Allieri,[a] F. Pioselli,[a] R. Angelucci,[b] A. Poggi,[b] A. Tagliani[b] and S. Nicoletti[b]

[a]Istituto Nazionale per la Fisica della Materia and Dipartimento di Chimica e Fisica per l'Ingegneria e per i Materiali, Universitá di Brescia, Via Valotti, 9-25133 Brescia, Italy
[b]C.N.R. LAMEL Institute, Via Gobetti, 101-40129 Bologna, Italy

(Received 12 October 1998; accepted 10 February 1999)

Abstract

The effect of V on the microstructural properties of SnO_2 nanopowders is studied by performing X-ray diffraction, Raman spectroscopy and scanning electron microanalysis. The peak broadening in the diffraction data is interpreted in terms of crystallite size and microstrain effects and related to the presence of V ions within the lattice. After calcination at high temperatures, the decrease of microstrains and the increase in the average crystallite size is ascribed to V segregation as oxide. Though the amount of segregated V oxide is not detectable by X-ray diffraction, V_2O_5 is clearly detected by Raman measurements. © *1999 Published by Elsevier Science Limited. All rights reserved*

Keywords: SnO_2, calcination, powders-chemical preparation, X-ray methods, Raman spectroscopy.

1 Introduction

The development of supported metal oxide catalysts and metal oxide-based solid state gas sensors has greatly benefited from the microstructural studies aimed to point out the structural evolution of materials with annealing treatments. Based on these studies the structural evolution in terms of microstrains, particle size, phase segregation, and phase transitions is usually described.

When dealing with nanopowders materials, one is forced to take into account not only the bulk effects but also the surface properties which gain increasing importance with the increase of surface-to-volume ratio.

One of the system where all these aspects are strictly related is the Sn–V–O system. Far from being fully clarified, the doping of SnO_2 cassiterite with V or attempts to sintetize mixed V–Sn oxides still deserves a considerable work in which microstructural studies may play a major role.

While several authors have postulated the formation of solid solutions by way of diffusion of V ions into the SnO_2 lattice, and the formation of solid solutions has been ascertained, only few indications are available about the maximum V content in the cassiterite matrix.[1] The presence of microstrains and reduced grain size of V_xSnO_{2-x}, with respect to pure SnO_2 can be assumed as an evidence of V diffusion into cassiterite. Therefore information on the mechanisms of the reciprocal dissolution of V and Sn oxides can be drawn from a microstructural analysis.

The present study is aimed to characterize the effect of temperature on the stability of V_xSnO_{2-y} nanopowders. It is shown that vanadium enters the SnO_2 lattice and inhibits the crystallite growth at 700°C. However, excess VO_x, oxides are already detected at 700°C by Raman spectroscopy. At 900°C, vanadium segregates as V_2O_5, and increase of crystallite size and decrease of microstrains are observed.

2 Experimental

Pure and V-doped SnO_2 powders have been obtained by the coprecipitation method. Tin oxide powder has been prepared as follows: a 0·142 M solution of $SnCl_4$ in absolute ethyl alcohol has been added to a 2 M aqueous solution of NH_4CH_3COO. The tin-oxohydrate obtained has been dried at 150°C with a final calcination at 700°C in air for 1 h. Intermediate steps at 400 and 500°C

*To whom correspondence should be addressed.

have also been carried out in order to sublimate the NH_4Cl, the acetic acid and acetates which remained in the solid. In the same way a vanadium doped tin oxide has been obtained by adding $VO(acac)_2$ to the ethanolic solution of $SnCl_4$ in amount required to get a 10% atomic ratio of vanadium in the final material.

Upon a microstructural characterization of the powders calcinated at 700°C, the samples have been annealed in air for 1 h at 800°C and 900°C and characterized after each calcination step.

The structural investigation was performed by microraman spectroscopy and X-ray diffraction (XRD) and scanning electron microscopy. Microraman spectra were collected by a Dilor Labram spectrograph. The exciting source was a HeNe laser (632.8 nm) with a power of less than 10 mW at the sample. The microscope was coupled confocally to the spectrograph. A 100×NA 0·9 objective and a confocal hole opened at 400 μm were used. Rejection of the exciting line was obtained with a holographic notch filter.

XRD patterns were collected by a Philips MPD 1880 powder diffractometer with a graphite monochromated Cu k_α radiation in the Bragg–Brentano parafocusing geometry.

The profiles of the diffraction peaks were Fourier analysed by using a program developed by Lutterotti and Scardi (the calculations were performed by using the programs general peak separation routine MARQFIT[2a] and line broadening analysis[2b] based on single order methods.[3] The instrumental function, to be deconvoluted from the observed profile, was determined by measuring the diffraction pattern of a standard KCl powder and the micro-structural parameter $\langle M \rangle$ (average crystallise size) and $\langle \varepsilon^2 \rangle^{1/2}$ (mean-square root microstrains) were evaluated.

SEM images have been collected with Philips XL30 Scanning Electron Microscope.

3 Results and Discussion

Figure 1 shows the X-ray diffraction patterns of pure [Fig. 1(a)] and doped [Fig. 1(b)] SnO_2 powders taken after annealing at 700°C. The width of the reflections is larger for the doped powder, which indicates that in the doped sample either smaller crystallites or higher microstrains, or both are present. The reflections in the pattern were indexed by those of SnO_2 cassiterite. No reflections from V oxide phases are detected within the instrumental sensitivity. The XRD patterns collected from the two samples at 800 and 900°C, not reported here, have been analysed in order to characterize their microstructural properties. The

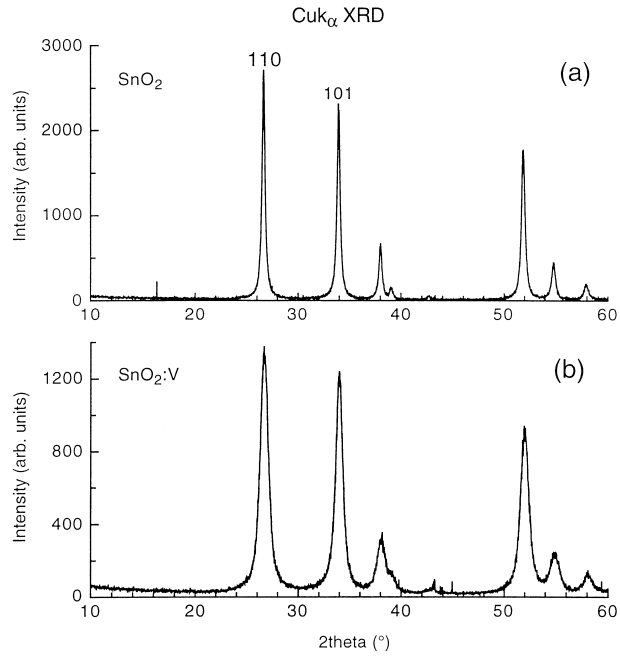

Fig. 1. X-ray diffraction pattern of the (a) pure and (b) V-doped SnO_2 powders treated at 700°C for 1 h.

data analysis (see discussion below and Fig. 3) was focussed on the two low-theta reflections at about 26·6° (110) and 33·95° (101). In all cases, only SnO_2 (cassiterite phase) was detected in the XRD patterns.

Figure 2 shows the Raman spectra of pure and doped SnO_2 powders taken after annealing at 700, 800, and 900°C. In all spectra, the A_{1g}, mode of SnO_2 cassiterite[4] is detected at about 630 cm^{-1}, and in the pure samples [Fig. 2(a)–(c)], other Raman active modes (E_g and B_{2g}) can be detected. By comparing the evolution of Raman spectra with temperature for the pure sample, one can observe that the temperature dependence of the SnO_2 Raman active modes well compares with that of XRD pattern, i.e. the Raman band gets narrower as the temperature increases, which also in the case of Raman spectroscopy usually indicates an increase of crystallite size (e.g. Ref. 5). The same holds for the SnO_2 Raman active modes of the V-doped samples.

In addition, for the V-doped samples, unlike XRD, the presence of V oxides can be evidenced from Raman spectra. The sample treated at 700°C shows a rather complex Raman spectrum [Fig. 2(d)]. As expected, the width of the peak corresponding to the A_{1g} mode of SnO_2, is large, but several additional bands have to be identified. One band at about 1000 cm^{-1} is clearly detectable. This band is quite close to the band ascribed to the V=O stretching mode in V_2O_5.[6] Nevertheless other Raman active modes of V_2O_5 are missing, such as the lattice mode at 143 cm^{-1}. This may indicate that metal–oxygen complexes with V=O

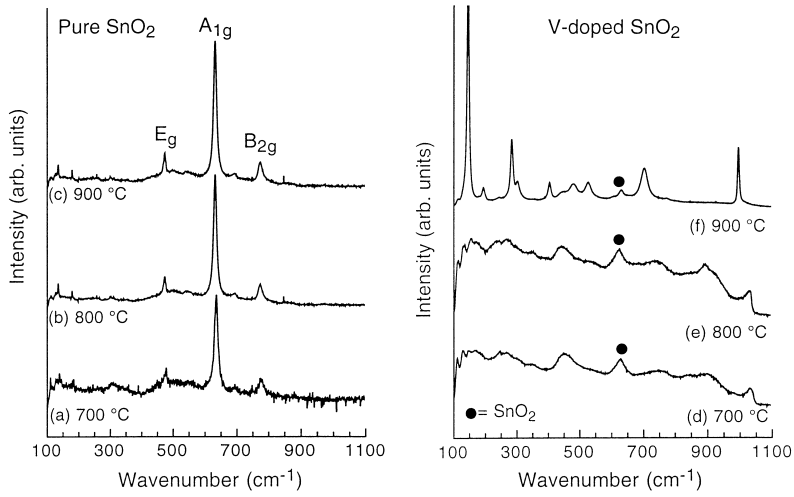

Fig. 2. Raman spectra of (a, b, and c) pure and (d, e, and f) V-doped SnO_2 powders treated at different temperatures. The dotted line above the (f) spectrum is an expanded view of (f).

coordination (i.e. apical oxygen) can be found in the powders but long range ordering of the V_2O_5 lattice is still missing. This situation remains unchanged also at 800°C [Fig. 2(e)]. Only at 900°C vanadium segregates as V_2O_5, as is clearly detectable in Fig. 2(f). The band at about 1000 cm^{-1} also has a temperature dependence which resembles that of TiO_2-supported V_2O_5, where the V=O stretching mode moves towards lower frequency and increases its intensity as the weight of V in the Ti–V–O material increases. Only above a certain V content the mode at 997 cm^{-1} of V_2O_5 is fully established (Ref. 7 and references, therein).

From Raman spectroscopy results we can therefore point out that: (i) the SnO_2 peaks of V-doped powders are larger than those of pure powders, which seems to indicate the presence of V within the lattice with the effect of limiting the growth of crystallites; (ii) the shape of the band at about 1000 cm^{-1} is typical of poorly crystallized VO_x complexes with terminal O atoms usually described either as as a two-dimensional polymeric network of distorted octahedra or surface vanadia species;[8] (iii) at 900°C the V_2O_5 phase is clearly detected, which seems to indicate the segregation of V out of the SnO_2 lattice.

The microstructural characterization was further carried out by calculating, on the basis of the XRD data, the evolution of the average grain size and microstrains with temperatures. The results are shown in Fig. 3.

The average grain size $\langle M \rangle$ [Fig. 3(a)] increases with increasing annealing temperature. Though the increase for pure SnO_2 is relatively low, V-doped SnO_2 shows a more remarkable increase above 800°C which may indicate possible segregation effects, similar to those observed for V-doped TiO_2.[9] The segregation Of V_2O_5 is confirmed by the microRaman spectroscopy data [Fig. 2(f)].

Also for microstrain $\langle \varepsilon \rangle^{1/2}$ [Fig. 3(b)], the variation with temperature is more pronounced for the V-doped powders. In both cases, microstrains decreases with annealing temperature. While for both 110 and 101 reflections the $\langle M \rangle$ value is the same at each temperature, relevant differences are found in microstrains. Indeed, microstrains calculated for the 110 reflections are higher than those calculated for the 101 reflection. This can be justified by the fact that the (110) plane contains the axis of the $[SnO_6]^{8-}$ edge-sharing octahedra chain, while the distance between (101) planes depends on the c-axis length. Since the chains of

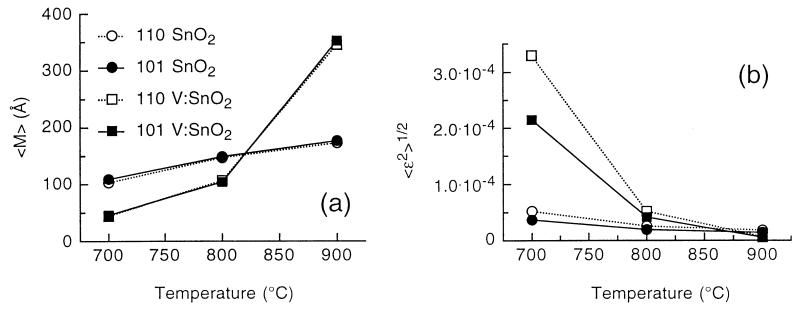

Fig. 3. Average crystallise size $\langle M \rangle$ and microstrain $\langle \varepsilon^2 \rangle^{1/2}$ calculated from the 110 and 101 reflections for both pure and V-doped powders.

octahedra running along the c-axis are stiff, the elastic module for the (101) family plane must be higher than that of the (110) family of planes.

Rather interesting is the fact that at 900°C the average grain size of the doped powder is larger than that of the pure powder. This finding is in agreement with the results of SEM data shown in Fig. 4. As can be observed the size of the agglomerates [Fig. 4(a)] of the pure powder at 900°C is clearly smaller than that of the doped powder [Fig. 4(b)] treated at the same temperature. However, it should he remarked that, as compared to the values of $\langle M \rangle$ estimated from diffraction data, the agglomerates appearing in the SEM micrographs are larger and can, in principle, have a polycrystalline nature.

On the basis of the measure of the 2θ angle corresponding to the 200 and 002 reflections of the X-ray diffractograms, the ratio between the distances of the pure and doped samples was calculated and reported in Table 1. The ratio between these distances corresponds to the ratio between the *a* and *c* unit cell axes. As can be observed, at all temperatures the ratio between the d_{002} distances ($=c/2$) are always greater that the ratio between the d_{200} distances ($=a/2$). Only at 900°C this ratio decreases for both axes and the two values become very close to each other. The fact that the ratio between *c* axes is larger than the ratio between the *a* axes can be ascribed to the presence of V in the SnO_2, lattice, which is supposed to determine a contraction of the *c* axis of the doped powder. Indeed, the *c* axis is parallel to the chains composed of edge-sharing metal–oxygen octahedra and the distance between octahedra determines the length of *c* axis. When the vanadium cation substitutes, as V^{4+}, the larger Sn^{4+} cation in the octahedra, a contraction of the distance in the chain is expected.[10] Evidences of the presence of V^{4+} cations in powders prepared in the same way as that described in the present work was detected by electronic paramagnetic resonance (EPR).[1] The analysis of the present experimental data has also evidenced that, for all temperatures, the cell volumes of the doped sample are reduced with respect to the volumes of the pure SnO_2 powders.

Table 1. Calculated ratios between the lattice spacing of the pure (d_{hkl}) and doped [$d_{hkl(doped)}$] material corresponding to the hkl = 200 and 002 reflections of the XRD pattern

	T = *700°C*	T = *800°C*	T = *900°C*
$d_{200}/d_{200(doped)}$	1.0015	1.0021	1.0006
$d_{002}/d_{002(doped)}$	1.0024	1.0064	1.0004

We can therefore conclude that V ions are located inside the SnO_2 crystallites with the effect to produce microstrains in the structure and reduce the grain size with respect to the pure powders. The presence of V can also be inferred by the contraction of the *c* axis and cell volume, due to the smaller ionic ratio of V^{4+} with respect to Sn^{4+}.

The present results on the effect of calcination on the V–Sn–O powders are in agreement with those reported by Cavani *et al.*,[11] where X-ray photoemission and diffuse reflectance spectroscopy studies were carried out in order to investigate the nature of V phases upon calcination of V–SnO_2 powders prepared by the coprecipitation method. The authors show that temperatures of calcination higher than 700°C cause changes in the as-prepared V–SnO_2 system. The evolution of the XPS spectra was interpreted well by assuming (i) a surface enrichment in vanadium occurring at 900°C with the migration of V ions from the bulk to the surface of the catalyst, and (ii) a high-temperature induced adjustment of the oxygen sublattice with surface segregation of V^{5+} oxides and recovery of bulk SnO_2 at 1000°C.

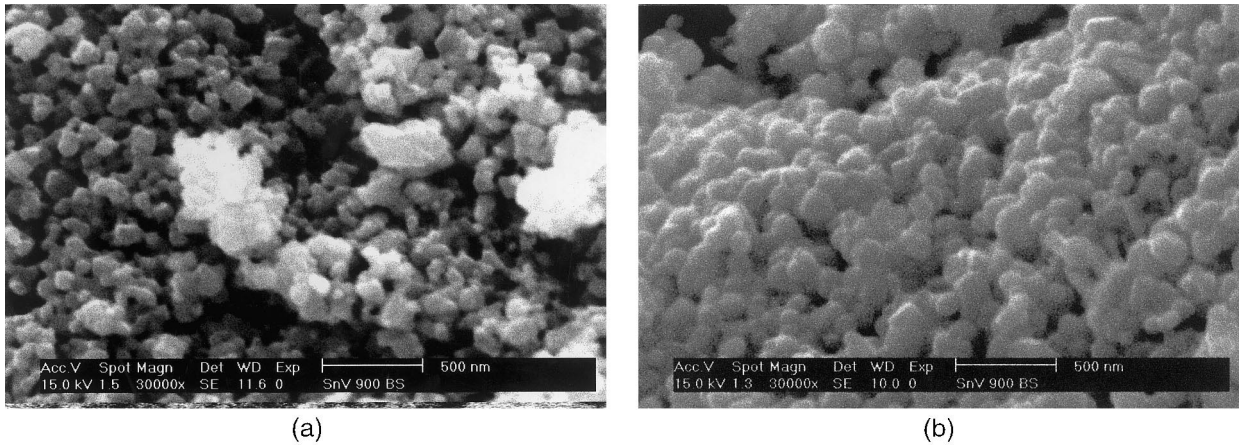

Fig. 4. SEM micrographs of the (a) pure and (b) doped powders treated for 1 h at 900°C.

Acknowledgements

This work was partially supported by the European Community under the ESPRIT Program 'SMOG'. C. Crivelli is acknowledged for the powder preparation and F. Cavani for helpful discussions.

References

1. Bordoni, S. Castellani, F. Cavani, F. Trifirò, F. and Gazzano, M., *J. Chem. Soc. Faraday Trans*., 1994, **90**, 2981.
2. a. Luterotti, L. and Scardi, P., *General Peak Separation Routine–MARQFIT*, 1990; b. W.A.X.S., *Line Broadening Analysis*, 1992.
3. Nandi, R. K., Kuo, H. K., Shosberg, W., Wissler, G., Cohen, J. B. and Crist, B., Jr, *J. Applied Cryst*, 1984, **17**, 22.
4. Peercy, P. S. and Morosin, B., *Phys. Rev. B*, 1973, **7**, 2779.
5. Nemanich, R. J., Solin, S. A. and Martin, R. M., *Phys. Rev. B*, 1981, **23**, 6348.
6. Benmoussa, M., Ibnouelghazi, E., Bennouna, A. and Amaziane, E. L., *Thin Solid Films*, 1995, **265**, 22–28.
7. Bond, G. C. and Flamerz Tahir, S., *Applied Catalysis*, 1991, **71**, 1–31.
8. Miyata, H., Tokuda, S. and Yoshida, T., *Appl. Spectr*., 1989, **43**, 522.
9. Depero, L. E., Bonzi, P., Musci, M. and Casale, C., *J. Solid State Chem*., 1994, **11**, 247.
10. Bolzan, A. A., Fong, C., Kennedy, B. J. and Howard, C. J., *Acta Cryst*., 1997, **B53**, 373.
11. Cavani, F., Trifirò, F., Bartolini, A., Ghisletti, D., Nalli, M. and Santucci, A., *J. Chem. Soc., Faraday Trans*., 1996, **92**, 9.